Available online at www.sciencedirect.com
SCIENCE DIRECT
Journal of Power Sources 154 (2006) 386–393
JOURNAL OF POWER SOURCES
www.elsevier.com/locate/jpowsour

Dynamic fuel cell models and their application in hardware in the loop simulation

Zijad Lemeš [a,*], Andreas Vath [b], Th. Hartkopf [b], H. Mäncher [a]

[a] *MAGNUM Automatisierungstechnik GmbH, Bunsenstr. 22, D-64293 Darmstadt, Germany*
[b] *Technische Universität Darmstadt/Institut für Elektrische Energiewandlung, Landgraf-Georg-Str. 4, D-64283 Darmstadt, Germany*

Available online 21 November 2005

Abstract

Currently, fuel cell technology plays an important role in the development of alternative energy converters for mobile, portable and stationary applications. With the help of physical based models of fuel cell systems and appropriate test benches it is possible to design different applications and investigate their stationary and dynamic behaviour. The polymer electrolyte membrane (PEM) fuel cell system model includes gas humidifier, air and hydrogen supply, current converter and a detailed stack model incorporating the physical characteristics of the different layers. In particular, the use of these models together with hardware in the loop (HIL) capable test stands helps to decrease the costs and accelerate the development of fuel cell systems. The interface program provides fast data exchange between the test bench and the physical model of the fuel cell or any other systems in real time. So the flexibility and efficiency of the test bench increase fundamentally, because it is possible to replace real components with their mathematical models.

Keywords: PEM fuel cell; Dynamic modelling; Hardware in the loop; Test benches; Simulation

1. Introduction

In the recent years there was an increasing interest in fuel cell technology. In particular, the polymer electrolyte membrane (PEM) fuel cell has reached a high development status. This development was mostly advanced by the automotive industry, because fuel cells are suitable to substitute the fossil fuels and also to provide an environment-friendly propulsion. But there is also a growing market for stationary fuel cell applications, e.g. for cogeneration of heat and power (CHP), and as a substitute for batteries in portable devices, e.g. for laptops.

Despite the progress made in first realised fuel cell vehicle fleets and CHP units there is still lot of work to be done to bring fuel cells to the market. The reduction of still high costs has the biggest priority but the build up of hydrogen infrastructure is not less important. Furthermore, the durability and reliability of conventional systems has to be reached.

By means of mathematical modelling the development and design of fuel cell systems can be highly accelerated. There are many three-dimensional steady-state PEM fuel cell models [1–3] described in several papers. The results are the local concentrations, the water amount of the membrane and their influence on the current density [4,5].

In particular for automotive and portable applications, the knowledge of dynamic behaviour is of vital importance. Therefore, the PEM fuel cell model which is presented in this work is capable of predicting the dynamic fuel cell behaviour depending on the operating conditions.

The use of test benches, which can be combined with the mathematical models of the components that are not available, opens up fully new possibilities in the development of fuel cell systems. The test benches, which are represented in this work, dispose a hardware in the loop (HIL) interface that provides fast data exchange between the test system with the available hardware to the models of those hardware which is not available.

As a result, the behaviour of a fuel cell system with dynamic loads is calculated with respect to voltage drops, humidification of the membrane, stack temperature and the influence of temperature on the reaction. Afterwards, the efficiency and the maximum performance of the fuel cell stack and of the whole system are analysed under different conditions. Finally, an application example of the HIL simulation is shown.

* Corresponding author. Tel.: +49 6151 802 568; fax: +49 6151 802 600.
E-mail address: zijad.lemes@magnum.de (Z. Lemeš).

0378-7753/$ – see front matter © 2005 Elsevier B.V. All rights reserved.
doi:10.1016/j.jpowsour.2005.10.032

Nomenclature

A_{Cell}	cell area (m^2)
C_{cool}	heat capacity ($J\,kg^{-1}\,K^{-1}$)
C_D	double layer capacitance (F)
j	current density ($A\,cm^{-2}$)
m_{cell}	cell mass (kg)
$N_{H_2,Mem}$	hydrogen transport in membrane ($mol\,s^{-1}$)
$N_{H_2O,Mem}$	water transport in membrane ($mol\,s^{-1}$)
$N_{i,GDL}$	molar flow gas diffusion layer ($mol\,s^{-1}$)
$N_{N_2,Mem}$	nitrogen transport in membrane ($mol\,s^{-1}$)
$N_{O_2,Mem}$	oxygen transport in membrane ($mol\,s^{-1}$)
p_i	partial pressure of component i (Pa)
P_{Th}	thermal power (W)
R_{El}	electrical resistance ($\Omega\,cm^2$)
R_{Mem}	ionic resistance ($\Omega\,cm^2$)
T	cell temperature (K)
T_{Air}	air temperature (K)
$T_{cool,in}$	temperature of cool medium (K)
U_{An}	anode voltage loss (V)
U_{Ca}	cathode voltage loss (V)
U_{cell}	cell voltage (V)
U_Ω	ohmic voltage loss (V)
V_{cool}	cool medium flow ($m^3\,s^{-1}$)
$y_{H_2,An}$	H_2 in the catalytic layer anode ($mol\,m^{-3}$)
$y_{H_2,Ca}$	H_2 in the catalytic layer cathode ($mol\,m^{-3}$)
$y_{H_2O,An}$	H_2O in the catalytic layer anode ($mol\,m^{-3}$)
$y_{H_2O,Ca}$	H_2O in the catalytic layer cathode ($mol\,m^{-3}$)
$y_{i,FF}$	component i in the flowfields ($mol\,m^{-3}$)
$y_{i,GDL}$	component i in diffusion layers ($mol\,m^{-3}$)
$y_{N_2,An}$	N_2 in the catalytic layer anode ($mol\,m^{-3}$)
$y_{N_2,Ca}$	N_2 in the catalytic layer cathode ($mol\,m^{-3}$)
$y_{O_2,An}$	O_2 in the catalytic layer anode ($mol\,m^{-3}$)
$y_{O_2,Ca}$	O_2 in the catalytic layer cathode ($mol\,m^{-3}$)
α_{Ca}	cathode charge transfer coefficient
δ_{Mem}	swelling factor of the membrane
ε_i	porosity of medium i
λ	stoichiometry of gas supply

2. Fuel cell system model

The dynamic fuel cell system model (Fig. 1) includes hydrogen and air supply, humidifier, consumer load, electrical energy storage, cooling system and a detailed stack model. The model has been implemented in MATLAB/Simulink software and the simulation can run with discrete or continuous time steps.

The air and hydrogen are humidified to the set values before they reach the stack. The pressure and the flow rate are controlled by the check valve and the compressor. The cooling system can be based on a liquid or gaseous medium. If the current or the power for the consumer load is set, the voltages of the stack and of the electrical energy storage are calculated. With the help of the regulation/control system it is possible to test a lot of different operation strategies and the power split-up between the stack and the energy storage. A further advantage is that the system model can be changed easily because it is built out of different autonomous operating blocks.

In the following the description of the stack model is given; the description of the entire fuel cell system is not the subject of this work.

2.1. Stack model

In the one-dimensional stack model the different layers (Fig. 2) are implemented with their different physical and electrochemical characteristics. In the diffusion layer and the catalyst layer the transport mechanism of hydrogen, nitrogen, oxygen, water vapour and liquid water is included. The water transport through the membrane incorporates the effects of concentration gradients and the electro-osmotic drag. The nitrogen and hydrogen transport through the membrane is also included.

After calculation of partial pressures of the gaseous species, the water amount in the different layers, the polarisation losses at anode and cathode and the membrane voltage loss are calculated. The polarisation losses are calculated under consideration of the double layer capacitance at the electrodes. The outcome of the model is the stack voltage and the electrical power. The thermal power, the stack temperature and the rejected heat are computed under the condition that the temperature of all cells is uniform. The existing gas volumes in the stack have a big influence on the performance especially for dynamic loads, varying gas supply or gas humidifying. The most important input and output parameters are listed in Table 1.

The gas diffusion layer is modelled as a porous media, which is usually made out of carbon. For the diffusion processes it is necessary to calculate the amount of liquid water in this media because at certain operation conditions the pores get filled with water and the diffusion process of the gases decreases (Table 2).

Also, the parameters and properties of catalyst layers and the membrane are summarised in Tables 3 and 4.

An overview of all above-mentioned different layers and parts of a fuel cell is shown in Fig. 2.

Table 1
Stack parameters

	Stack
Parameters	Cell area
	Number of cells in the stack
	Heat capacity
	Gas volume anode
	Gas volume cathode
	Initial conditions (temperature, gas composition, pressure)
Input	Load current/power
	Cooling medium (type, temperature, flow rate)
	Gas inlet (pressure, flow rate, temperature, composition)
Output	Voltage/current
	Cooling medium (temperature)
	Gas outlet (pressure, flow rate, temperature, composition)

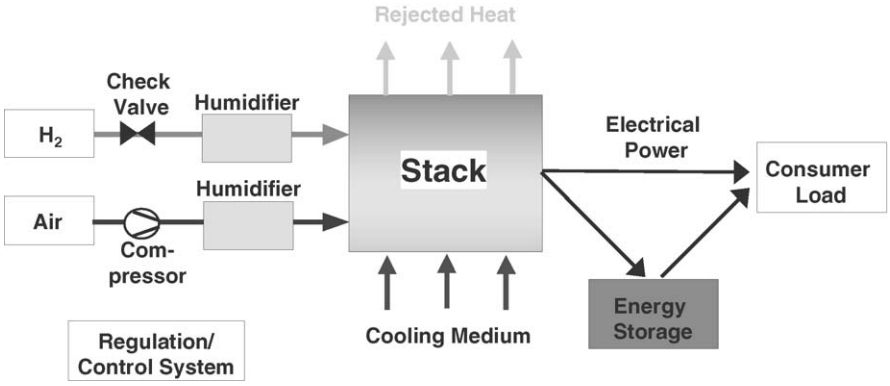

Fig. 1. Fuel cell system model.

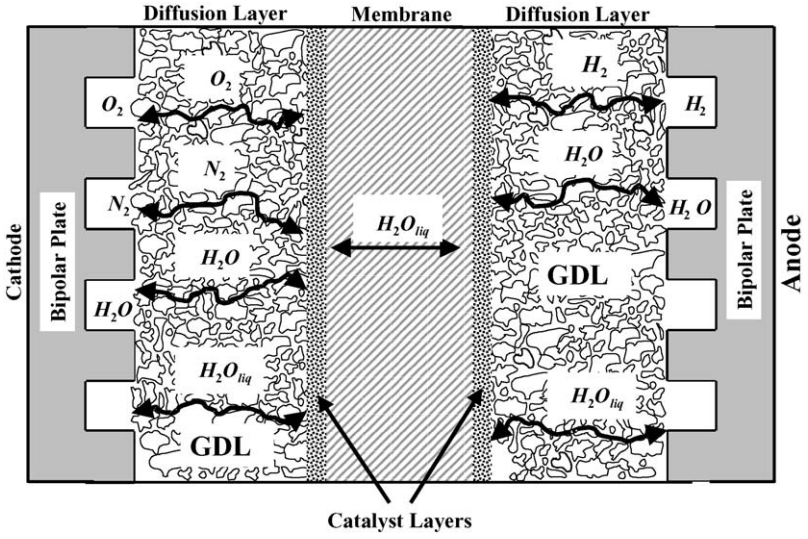

Fig. 2. Different layers within a fuel cell.

2.2. Main relations incorporated in the dynamic fuel cell model

The general dependencies of modelled values are given in Section 2.2.1, then a more detailed description of cell voltage is given in particular regarding the double layer capacitance.

Table 2
Gas diffusion layers

	Gas diffusion layer
Structure	Porous media
Transported species	Anode gases (H_2, H_2O_gas, H_2O_liq) Electrons Cathode gases (N_2, O_2, H_2O_gas, H_2O_liq)
Phenomena	Gas transport because of diffusion and convection Liquid and gaseous water transport Porosity depends on the amount of liquid water
Parameters	Thickness Porosity Diffusion coefficients for H_2O_gas, H_2O_liq, N_2, O_2 and H_2

Cell voltage:

$$U_{\text{cell}} = f(T, p_i, \lambda, y_{\text{H}_2,\text{An}}, y_{\text{O}_2,\text{Ca}}, y_{\text{H}_2,\text{Ca}}, y_{\text{O}_2,\text{An}}, j, A_{\text{Cell}}, C_{\text{D}})$$

Cell temperature:

$$T = f(P_{\text{Th}}, T_{\text{cool,in}}, V_{\text{cool}}, C_{\text{cool}}, m_{\text{cell}}, \text{stack size}, T_{\text{Air}})$$

Table 3
Catalyst layers

	Catalyst layer
Structure	Porous media, mixture made of the membrane and backing layer material and catalyst particles
Transported species	Anode gases (H_2, H_2O_gas, H_2O_liq) Electrons Cathode gases (N_2, O_2, H_2O_gas, H_2O_liq)
Phenomena	Double layer capacitance Electrochemical reaction Water production at the cathode
Parameters	Thickness Porosity Exchange current densities for anode and cathode Diffusion coefficients for H_2_gas, H_2O_liq, N_2, O_2 and H_2

Table 4
Membrane

	Membrane
Structure	Polymeric, commonly made of Nafion®
Transported species	Protons Water Permeable to hydrogen and oxygen
Phenomena	Proton transport Water transport due to diffusion, hydraulic pressure and the drag effect of the hydrogen ions Swelling Proton conductivity as a function of the membrane humidity Diffusion through the membrane H_2O_liq, N_2, O_2 and H_2
Parameters	Thickness Number of SO_3H Diffusion coefficients for H_2O_liq, N_2, O_2 and H_2

Gas transport within the diffusion media:

$$N_{i,\mathrm{GDL}} = f(T, p_i, y_{i,\mathrm{FF}}, y_{i,\mathrm{GDL}}, j, A_{\mathrm{Cell}}, \varepsilon_i)$$

Herein, ε is a function of the amount of water in the according media.
Water transport within the membrane:

$$N_{\mathrm{H_2O,Mem}} = f(T, p_i, y_{\mathrm{H_2O,Ca}}, y_{\mathrm{H_2O,An}}, j, A_{\mathrm{Cell}}, \delta_{\mathrm{Mem}})$$

Oxygen transport within the membrane:

$$N_{\mathrm{O_2,Mem}} = f(T, p_i, y_{\mathrm{O_2,Ca}}, y_{\mathrm{O_2,An}}, j, A_{\mathrm{Cell}}, \delta_{\mathrm{Mem}})$$

Hydrogen transport within the membrane:

$$N_{\mathrm{H_2,Mem}} = f(T, p_i, y_{\mathrm{H_2,Ca}}, y_{\mathrm{H_2,An}}, j, A_{\mathrm{Cell}}, \delta_{\mathrm{Mem}})$$

Nitrogen transport within the membrane:

$$N_{\mathrm{N_2,Mem}} = f(T, p_i, y_{\mathrm{N_2,Ca}}, y_{\mathrm{N_2,An}}, j, \delta_{\mathrm{Mem}})$$

2.2.1. Cell voltage

The cell voltage is described by the following equation:

$$U_{\mathrm{cell}} = U_0 - U_{\mathrm{An}} - U_{\Omega} - U_{\mathrm{Ca}} \tag{1}$$

where U_0 is the open cell voltage, U_{An} and U_{Ca} the voltage losses on anode and cathode side and U_{Ω} represents the ohmic losses due to ionic conductivity of the membrane and due to electronic conductivity of bipolar plates, diffusion and catalyst layers.

The open cell voltage is a function of temperature and partial pressures of reactants and is calculated as follows:

$$U_0 = -\frac{\Delta G^0}{2F} + \frac{\Delta S}{2F}(T - T^0) + \frac{RT}{2F}\left(\frac{1}{2}\ln\frac{p_{\mathrm{O_2}}}{p^0} + \ln\frac{p_{\mathrm{H_2}}}{p^0}\right) \tag{2}$$

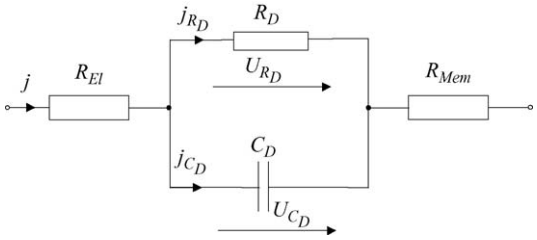

Fig. 3. Equivalent circuit of a double layer.

Based on the Butler–Volmer-Equation [6] which describes the reduction and oxidation processes on the electrode and neglecting the opposite reaction on each electrode (Tafel-Equation [6,7]), the losses through the charge transfer can be described as follows:

$$U_{\mathrm{Ca}} = \frac{R \cdot T}{\alpha_{\mathrm{Ca}} \cdot F} \cdot \ln\frac{j}{j_{0,\mathrm{Ca}}} \tag{3}$$

The exchange current density j_0 and transfer coefficient α are measures for the reaction kinetic. The exchange current density is concentration and temperature dependent. Because of the considerably higher exchange current density for the hydrogen electrode the charge transfer losses on the anode side can be neglected.

The ohmic losses are given by the following equation:

$$U_{\Omega} = R_{\mathrm{El}} \cdot j + R_{\mathrm{Mem}} \cdot j \tag{4}$$

where R_{El} represents the losses through the electronic conductivity and R_{Mem} is the voltage loss due to ionic conductivity of the membrane. The conductivity of the membrane depends on temperature and water content [8].

Regarding the fast load changes it is of high interest to know the voltage response and the storage capacity of a double layer. Fig. 3 shows the equivalent circuit of the double layer and the corresponding resistances.

In this case the double layer is modelled as the parallel connection of double layer capacitance and charge transfer resistance. With Fig. 3 and Eq. (3) following relationships are given:

$$U_{R_{\mathrm{D}}} = U_{C_{\mathrm{D}}} = U_{\mathrm{Ca}} = \frac{RT}{\alpha_{\mathrm{Ca}} F}\ln\left(\frac{j_{R_{\mathrm{D}}}}{j_{0,\mathrm{Ca}}}\right) \tag{5}$$

$$j_{C_{\mathrm{D}}} = C_{\mathrm{D}} \cdot \frac{\mathrm{d}U_{C_{\mathrm{D}}}}{\mathrm{d}t} \tag{6}$$

Using Kirchhoff's first law and Eqs. (5) and (6) following differential equation for the cathode voltage is obtained:

$$\frac{\mathrm{d}U_{\mathrm{Ca}}}{\mathrm{d}t} = \frac{j}{C_{\mathrm{D}}} - \frac{j_{0,\mathrm{Ca}}}{C_{\mathrm{D}}} \cdot \exp\left(\frac{U_{\mathrm{Ca}}}{K}\right) \tag{7}$$

with:

$$K = \frac{RT}{\alpha_{\mathrm{Ca}} F} \tag{8}$$

Because of the low charge transfer resistance also the resulting time constant is small so that the double layer capacitance on the anode side can be neglected.

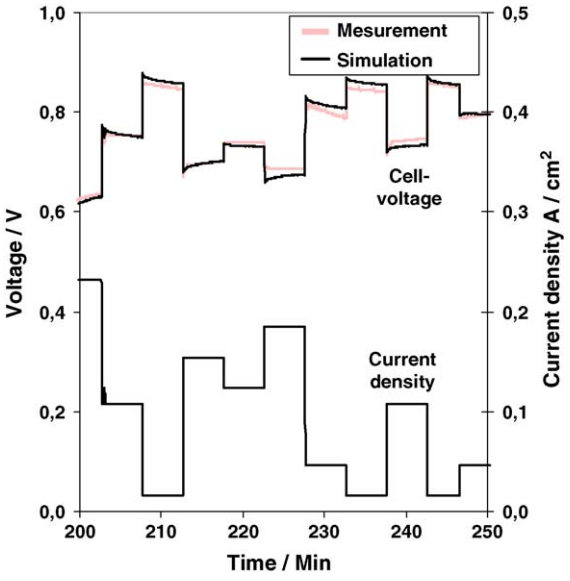

Fig. 4. Cell voltage at dynamic load current changes.

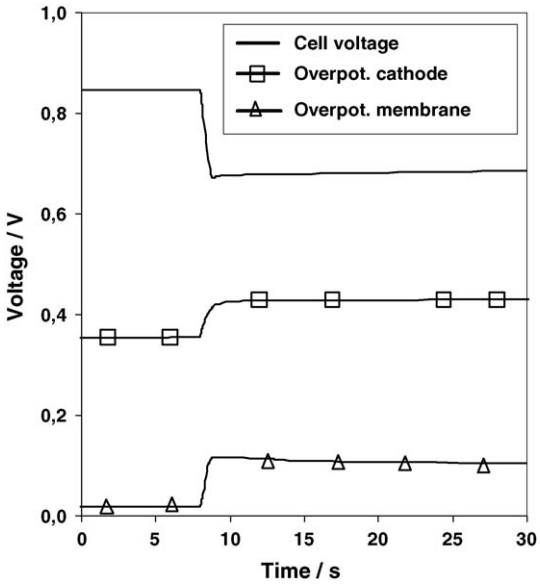

Fig. 6. Simulated voltage losses according to dynamic excitation in Fig. 4.

2.3. Simulation results

In this section the dynamic behaviour of the fuel cell model is shown and compared with the measurements of a stack. The stack was air cooled and the gases at the inlet were not humidified during the measurement to see the influence of the membrane resistance during operation.

In Fig. 4 the cell voltage of the simulation is compared with measured values for dynamic loads. There is an excellent conformance at dynamic loads between the simulated and measured stack voltage. The same load characteristics as in Fig. 4 are based on Figs. 5–7.

Fig. 5 shows the results of calculation of the different overpotentials and the cell voltage. The cathode overpotential has similar characteristic as the current density shown in Fig. 4. The anode overpotential has similar characteristic as the cathode overpotential but its amplitude is very low. The membrane voltage loss depends on the current density and the proton conductivity. Because of the linear correlation between current density and membrane resistance for a current density increase there is a high initial increase in the membrane overpotential. Later on, the resistance is decreasing because of the water production in the stack and the initially nearly dry membrane is now moistened (see also Fig. 7).

In Fig. 6 the overpotential for a decrease in current density from 15 mA cm^{-2} to 150 mA cm^{-2} is blown up. In this case the cathode overpotential does not increase by a step because of the capacitive double layer. The discharge of this layer takes a few seconds and during this time the overpotential increases

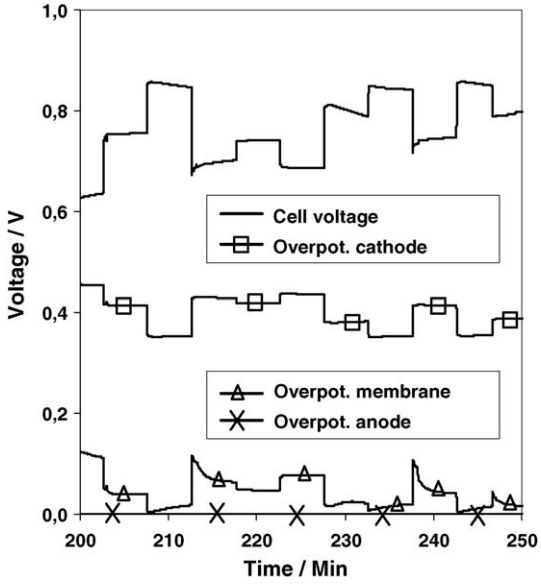

Fig. 5. Simulated voltage losses according to dynamic excitation in Fig. 4.

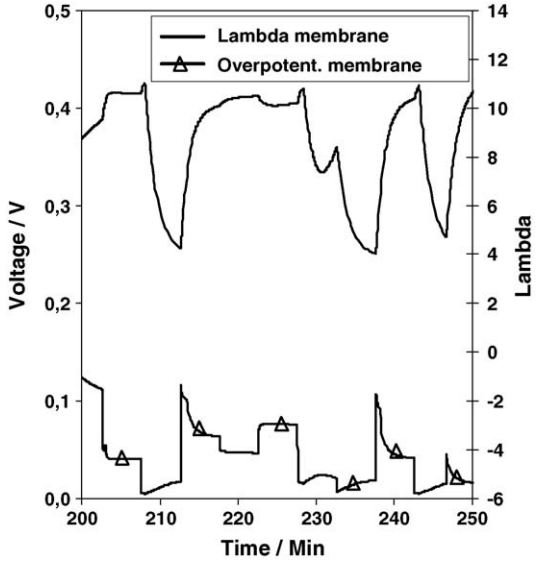

Fig. 7. Simulated membrane overpotential and humidity according to dynamic excitation in Fig. 4.

following the characteristics of an exponential function. The decrease in the oxygen partial pressure results in an overpotential increase.

In Fig. 7 the characteristic amount of water and the corresponding membrane overpotential is shown. The membrane overpotential is the result of the current density and the proton conductivity which depends on the water content. The water content is characterised as Lambda, which is defined as the number of water molecules divided by the number of SO_3H molecules. When the current is low the production of water at the cathode is also low and the membrane gets dry and their resistance increases. Going to higher load steps the overpotential is initially very high because of the dryness of the membrane. After some time the membrane becomes more wet and the resistance decreases.

3. HIL test benches

For the development of fuel cell stacks or fuel cell systems, there is an increasing need in suitable test benches. The MAGNUM company has been one of the first suppliers of fuel cell test benches and in particular of HIL capable test benches. The advantage of using HIL test stands is that in early stage of development testing of whole system can be performed, even if all the hardware is not available. Fig. 8 shows the configuration of a conventional test stand.

As shown in Fig. 8 the whole fuel cell system can only be tested if all sub-systems and units are available. In contrast, Fig. 9 shows the configuration if there is a possibility to integrate HIL simulation.

As shown in Fig. 9 now it is possible to replace defective or not available components with their mathematical models

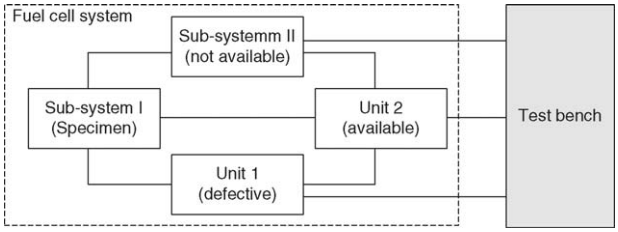

Fig. 8. Conventional test bench.

and perform analysis of operational behaviour of the fuel cell system.

Because of the possibility to operate the hardware together with simulation models one of the main aspects for the realisation of HIL test stands is the safety. This high safety standard is reached through the implementation of multistage switch off procedure on the PLC (Fig. 9). Further on, each of the set values for the controllers calculated in the model is checked for the plausibility by the PLC before being passed on to the hardware. The PLC will restrict the set values to reasonable limits and prevent dangerous operation conditions. This is especially important in case of, e.g. to mix hydrogen and oxygen on the anode side, or when the pressure set values were calculated by the model.

Another important aspect regarding automotive applications is the dynamic operation of the test bench. Therefore, fast mass flow and pressure controllers are integrated and also fast data acquisition and data exchange between the PLC and control PC, respectively, simulation PC are realised.

In order to afford dynamic changes of the gas humidification in the test stand, model based control algorithms are implemented. Thermodynamic simulations have been integrated to

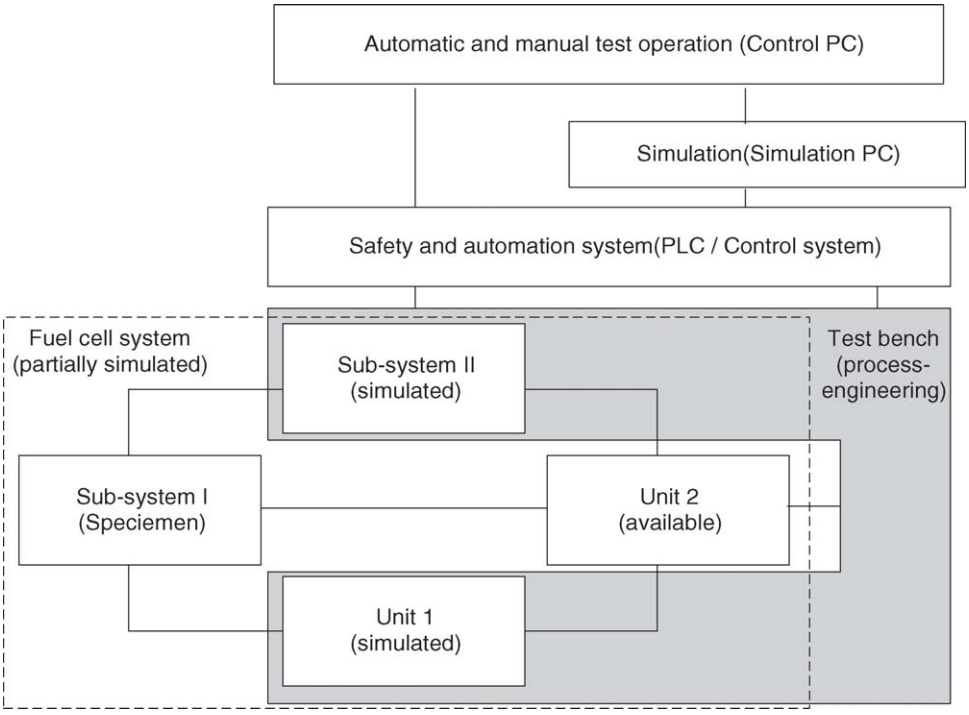

Fig. 9. HIL capable test bench.

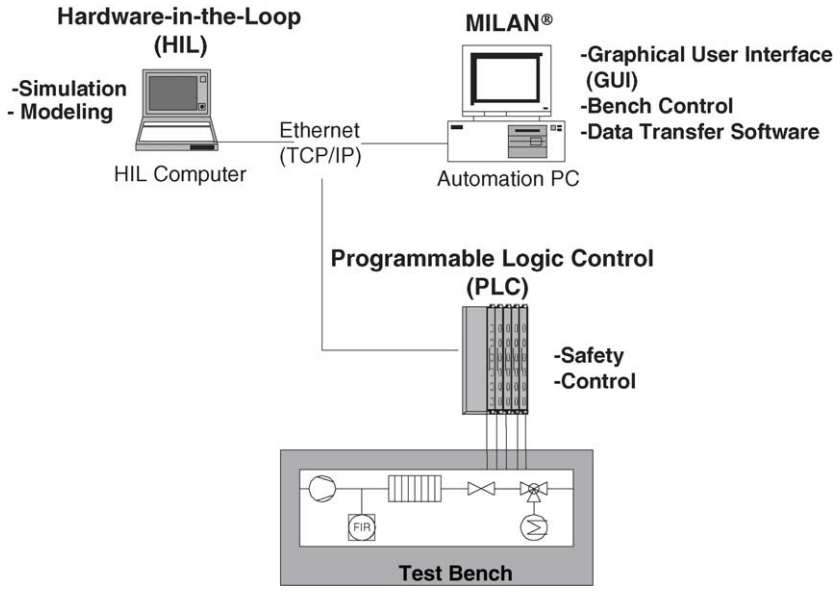

Fig. 10. Automation and data transfer within HIL test bench.

develop new control algorithms for temperature and moisture. These methods allow to determine the actual moisture with high accuracy, by measuring solely temperature and considering heat capacities of gases and equipment.

Fig. 10 gives an overview of the general configuration of the above described test bench and the interaction of the test stand with the control and simulation PC.

As shown in Fig. 10 the fast data transfer between the automation PC, HIL computer and the PLC is realised via ethernet connection. The HIL simulation can be started by the operator by choosing an adequate operation mode on the automation PC. The simulation model is running on the HIL PC in the real time writing selected set values to the PLC and simultaneously reading actual values from PLC.

3.1. Application examples

In the following two application examples of HIL simulations are presented. Because of the increasing interest of automotive industry on the fuel cell technology there is also an increasing need for testing of fuel cell powered cars. An example of how the HIL capable test bench can be used in the development process of fuel cell vehicle is shown in Fig. 11.

Fig. 12. FuelCell-HIL simulator.

In this example the test bench represents the power unit of the vehicle where in a fuel cell hydrogen together with oxygen is converted into electricity, which can be supplied to the electrical motor of vehicle propulsion unit. On the simulation PC the vehicle model is running in real time. Using this configuration (Fig. 11) static and dynamic behaviour of a power unit can be tested in an early development stage when the real vehicle is not available.

Next example shows how the above described stack model running on a real time target (Fig. 12) can be integrated in a surrounding system and can be used within HIL simulation for

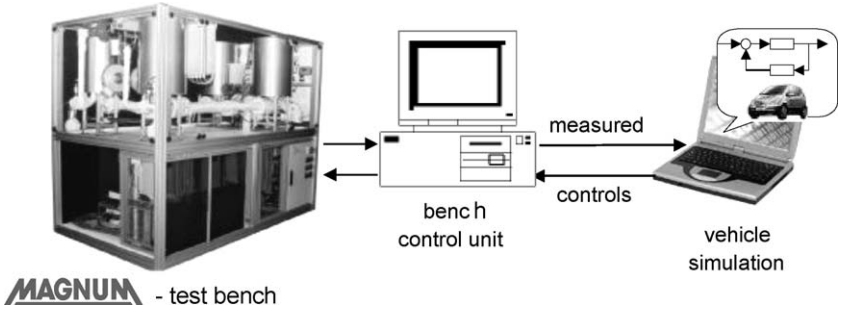

Fig. 11. HIL simulation of a fuel cell vehicle.

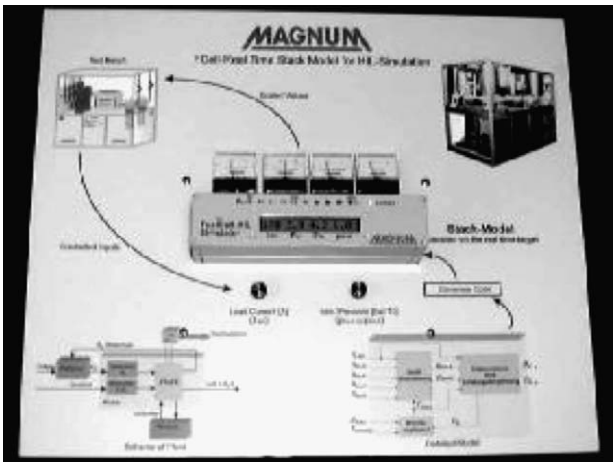

Fig. 13. Demonstration of a FuelCell-HIL simulator.

design of components and controls. In this case the real time target system acts as a stack dummy.

The FuelCell-HIL simulator shown in Fig. 12 can be connected to the surrounding system via the input and output ports and so the system behaviour can be analysed and controller design can be done when the real stack is not available. An application of the FuelCell-HIL simulator shown in Fig. 13 illustrates the interaction between the simulation and the hardware. For the demonstration purposes here the load current and the pressure can be changed by the user via potentiometer and the reaction of the stack can be observed. On the gauges the stack voltage, electrical and thermal power and stack temperature, which were calculated by the model, are shown.

4. Summary

A dynamic model of PEM fuel cell has been presented. In addition to the calculation of cell voltage this model is also capable of calculating time dependent temperature of the stack and partial pressures of the gaseous species. The voltage losses on the cathode are calculated considering the double layer capacitance.

The setup of HIL capable test benches has been shown and the special requirements for using these test benches for fuel cell testing have been described. The use of the HIL test benches together with simulation models and the resulting advantages for the development of fuel cell systems has been demonstrated.

References

[1] D. Benardi, W. Verbrugge, A mathematical model of the solid–polymer–electrolyte fuel cell, J. Electrochem. Soc. 139 (1992) 2477–2491.
[2] T. Springer, M. Wilson, S. Gottesfeld, Modelling and experimental diagnostic in polymer electrolyte fuel cells, J. Electrochem. Soc. 140 (1993) 3513–3526.
[3] A. Kazim, H. Liu, P. Forges, Modelling of performance of PEM fuel cells with conventional and interdigitated flow fields, J. Appl. Electrochem. 29 (1996) 1409–1416.
[4] F. Fuller, J. Newman, Water and thermal management in solid–polymer–electrolyte fuel cells, J. Electrochem. Soc. 140 (1993) 1216–1225.
[5] P. Costamagna, Transport phenomena in polymeric membrane fuel cells, Chem. Eng. Sci. 56 (2001) 323–332.
[6] H. Wendt, G. Kreysa, Electrochemical Engineering, Springer-Verlag, Berlin, Heidelberg, 1999.
[7] C.H. Hamann, W. Vielstich, Elektrochemie, 3, vollständig überarbeitete Auflage, Wiley/VCH Verlag, Weinheim, 1998, 3. Auflage.
[8] T.E. Springer, T.A. Zawodzinski, S. Gottesfeld, Polymer electrolyte fuel cell model, J. Electrochem. Soc. 138 (August (8)) (1991).